The Plant Cell, Vol. 20: 381–395, February 2008, www.plantcell.org © 2008 American Society of Plant Biologists

ROOT HAIR DEFECTIVE4 Encodes a Phosphatidylinositol-4-Phosphate Phosphatase Required for Proper Root Hair Development in *Arabidopsis thaliana* [W]

Julie M. Thole,[a] Joop E.M. Vermeer,[b] Yanling Zhang,[c] Theodorus W.J. Gadella Jr.,[d] and Erik Nielsen[a,c,1]

[a] Department of Biology, Washington University, St. Louis, Missouri 63130
[b] Section of Plant Physiology, Swammerdam Institute for Life Sciences, University of Amsterdam, 1098 SM Amsterdam, The Netherlands
[c] Department of Molecular, Cellular, and Developmental Biology, University of Michigan, Ann Arbor, Michigan 48109
[d] Section of Molecular Cytology, Swammerdam Institute for Life Sciences, University of Amsterdam, 1098 SM Amsterdam, The Netherlands

Polarized expansion of root hair cells in *Arabidopsis thaliana* is improperly controlled in root hair–defective *rhd4-1* mutant plants, resulting in root hairs that are shorter and randomly form bulges along their length. Using time-lapse fluorescence microscopy in *rhd4-1* root hairs, we analyzed membrane dynamics after labeling with RabA4b, a marker for polarized membrane trafficking in root hairs. This revealed stochastic loss and recovery of the RabA4b compartment in the tips of growing root hairs, consistent with a role for the RHD4 protein in regulation of polarized membrane trafficking in these cells. The wild-type *RHD4* gene was identified by map-based cloning and was found to encode a Sac1p-like phosphoinositide phosphatase. RHD4 displayed a preference for phosphatidylinositol-4-phosphate [PI(4)P] in vitro, and *rhd4-1* roots accumulated higher levels of PI(4)P in vivo. In wild-type root hairs, PI(4)P accumulated primarily in a tip-localized plasma membrane domain, but in *rhd4-1* mutants, significant levels of PI(4)P were detected associated with internal membranes. A fluorescent RHD4 fusion protein localized to membranes at the tips of growing root hairs. We propose that RHD4 is selectively recruited to RabA4b-labeled membranes that are involved in polarized expansion of root hair cells and that, in conjunction with the phosphoinositide kinase PI-4Kβ1, RHD4 regulates the accumulation of PI(4)P on membrane compartments at the tips of growing root hairs.

INTRODUCTION

The establishment of polarity is an essential aspect of eukaryotic cellular differentiation and requires asymmetric delivery of membranes and proteins via membrane trafficking. While much is known about the organization of individual membrane trafficking pathways within cells, less is known about how they are regulated during cellular differentiation. We have focused specifically on the process of polarized membrane trafficking during the differentiation of epidermal root hair cells in *Arabidopsis thaliana*.

Arabidopsis root hairs are single cells that grow by targeted secretion of cell wall components to the growing tip of the cell (Schnepf, 1986; Dolan, 2001). In plants, polarized cell growth requires new cell wall deposition and is dependent upon polarized secretion of vesicle cargo, with Rab GTPases mediating the sorting and delivery of this cargo within the cellular membrane trafficking pathway. Rab GTPases function by recruiting cytosolic effector proteins to specific subcellular membranes to regulate aspects of membrane trafficking through those compartments (Zerial and McBride, 2001).

[1] Address correspondence nielsene@umich.edu.
The author responsible for distribution of materials integral to the findings presented in this article in accordance with the policy described in the Instructions for Authors (www.plantcell.org) is: Erik Nielsen (nielsene@umich.edu).
[W] Online version contains Web-only data.
www.plantcell.org/cgi/doi/10.1105/tpc.107.054304

We have previously shown that RabA4b, a plant Rab GTPase, is localized to membrane compartments at the tips of growing root hairs, where it functions to regulate polarized secretion (Preuss et al., 2004). We also recently reported that phosphatidylinositol-4 kinase β1 (PI-4Kβ1), a RabA4b effector protein, is necessary for proper root hair development (Preuss et al., 2006). Therefore, RabA4b and its effector PI-4Kβ1 are required for proper polarized secretion in root hairs in *Arabidopsis*. Similarly, interaction of Rab GTPases and phosphoinositide kinases has been shown in other systems: mammalian Rab11 interacts directly with PI4KIIIβ (de Graaf et al., 2004), and yeast Ypt31 interacts genetically with Pik1p (Sciorra et al., 2005).

In eukaryotic cells, particular phosphoinositides preferentially mark subcellular membranes and recruit phosphoinositide binding proteins, providing spatial and temporal cues within the cell (Bankaitis and Morris, 2003; Pendaries et al., 2005). In both yeast and animal cells, generation and turnover of phosphoinositide pools play important roles in regulation of membrane trafficking steps (De Matteis and Godi, 2004; Di Paolo and De Camilli, 2006). In particular, in animals, phosphatidylinositol-4,5-bisphosphate [PI(4,5)P_2] and phosphatidylinositol-3,4,5-trisphosphate [PI(3,4,5)P_3] play essential roles in cellular polarization in a number of differentiating cell types (Pinal et al., 2006; Martin-Belmonte et al., 2007; Nishio et al., 2007). In plants, PI(4,5)P_2 accumulates at the tips of growing pollen tubes and root hair cells (Kost et al., 1999; Vincent et al., 2005), and mutation of a phosphatidylinositol transfer protein results in shorter, branched root hairs (Bohme et al., 2004; Vincent et al., 2005). Also, phospholipase C (PLC) uses

PI(4,5)P_2 as a substrate, and mutations in PLC influence pollen tube growth and root hair growth (Fischer et al., 2004; Dowd et al., 2006).

Yeast Sac1p is an essential gene in yeast, and this gene has been characterized as a phosphatidylinositol-4-phosphate (PI(4)P) phosphatase (Hughes et al., 2000; Foti et al., 2001). The SAC phosphatase domain has been defined by the seven highly conserved motifs found in Sac1p (Hughes et al., 2000). Yeast also contains a second SAC domain–containing phosphatase, Fig4p, which is a PI(3,5)P_2 5-phosphatase (Rudge et al., 2004). SAC domains are also found in mammalian synaptojanins and the yeast homologs Inp52p and Inp53p. These proteins contain a 5-phosphatase domain in addition to their N-terminal SAC domain (Hughes et al., 2000).

The *Arabidopsis* genome contains nine SAC domain proteins, which can be separated into three classes: SAC1-5 are most similar to yeast Fig4p, SAC6-8 are most similar to yeast Sac1p, and SAC9 contains unique domains (Zhong and Ye, 2003). Thus far, only two of these have been characterized: The SAC1 protein has been shown to have PI(3,5)P_2 phosphatase activity, and mutation of the *SAC1* gene causes cell wall and actin cytoskeleton defects along with aberrant cell morphology (Zhong et al., 2005). Mutation of *SAC9* results in overaccumulation of PI(4,5)P_2 and induces expression of stress response genes (Williams et al., 2005). Less is known about the *SAC6-8* genes except that their cDNAs can rescue the yeast Sac1p mutation (Despres et al., 2003). Additionally, both a promoter-β-glucuronidase study and tissue-specific RT-PCR experiments (Despres et al., 2003; Zhong and Ye, 2003) demonstrate that *SAC7* and *SAC8* are expressed broadly, while *SAC6* is expressed only in pollen.

Previously, we found an altered localization of enhanced yellow fluorescent protein (EYFP)-RabA4b fusion protein in short bulged root hairs of the mutant *rhd4-1* (Schiefelbein and Somerville, 1990); EYFP-RabA4b was not observed in bulging root hairs in *rhd4-1* but appeared to be tip localized in root hairs with tip-restricted expansion or in those in which tip growth had reestablished from bulges (Preuss et al., 2004). Here, we use time-lapse fluorescence microscopy to show that tip localization of EYFP-RabA4b–labeled membrane compartments display altered dynamics in *rhd4-1* root hairs. Using map-based cloning techniques, we identified RHD4 as a Sac1p-like phosphoinositide phosphatase, previously named SAC7. In vitro experiments demonstrate that RHD4 displays selectivity for PI(4)P, and *rhd4-1* mutant plants contain increased levels of PI(4)P in root tissues. Correspondingly, by monitoring localization of a PI(4)P binding RHD fusion protein, we observed an altered localization of PI(4)P in *rhd4-1* root hairs. Based on these observations and the previous identification of a role for PI-4Kβ1 in tip growth, we propose that regulation of both PI(4)P levels and its subcellular distribution by RHD are important for proper organization of polarized secretion during root hair development.

RESULTS

Spatial and Temporal Distribution of RabA4b Is Altered in *rhd4-1* Root Hairs

Previously, we showed that the plant Rab GTPase, RabA4b, labeled membranes that accumulated at the tips of growing root hair cells in *Arabidopsis* (Preuss et al., 2004). To better understand the role of RabA4b in root hair development, we expressed a fusion of EYFP and RabA4b in a series of root hair mutant backgrounds (Preuss et al., 2004).

To determine if tip localization of EYFP-RabA4b–labeled membranes was tightly linked with reestablished tip-restricted expansion out of root hair bulges, we performed time-lapse fluorescence microscopy in both wild-type and *rhd4-1* root hairs. In wild-type root hairs, the localization and levels of EYFP-RabA4b membranes detected by fluorescence microscopy in the tips of growing root hairs remained consistent over time (Figures 1A and 1B; see Supplemental Movie 1 online). By contrast, the presence and levels of EYFP-RabA4b membranes detected in the tips of *rhd4-1* root hairs varied greatly over time (Figure 1C; see Supplemental Movie 2 online). In many cases, loss of tip-localized EYFP-RabA4b compartments correlated with bulge formation and impaired rates of elongation (Figures 1C and 1D, arrows). When tip growth resumed from these bulges, it was accompanied by the accumulation of tip-localized EYFP-RabA4b (Figure 1C and shaded region in Figure 1D).

When quantifying this type of growth, we observed a relationship between the rate of root hair elongation and the presence of florescence signal obtained from the EYFP-RabA4b compartment (Figure 1D). We have observed this type of altered localization in >20 root hairs, and we have shown the best example of this localization pattern. While it was not clear whether loss or recovery of the tip-localized RabA4b compartment was responsible for bulge formation, this stochastic loss and recovery of the tip-localized compartment was clearly associated with the halting and resumption of elongation of the root hair and the bulged phenotype. These results suggested that RHD4 may be involved in regulating either proper distribution and/or accumulation of tip-localized RabA4b compartments during polarized growth in these cells.

RHD4 Is a Sac1p-Like Phosphoinositide Phosphatase

Based on the spatial and temporal localization pattern of EYFP-RabA4b in *rhd4-1* root hairs, we hypothesized that RHD4 may play a role in coordinating delivery of cell wall materials to the tips of root hairs. To determine RHD4 function, we undertook a map-based cloning approach to identify the gene responsible for the *rhd4-1* mutation, which had previously been mapped to the lower arm of chromosome 3 (Wang et al., 2001). To determine the genetic location of the *RHD4* locus, a mapping population was generated by crossing *rhd4-1* with the *Arabidopsis* ecotype Landsberg *erecta*. Homozygous *rhd4-1* F2 seedlings were selected, and simple sequence length polymorphisms (SSLPs) and cleaved amplified polymorphic sequences (CAPS) were used for physical mapping of the *rhd4-1* locus to an ~100 kb region of chromosome 3 containing 60 predicted open reading frames (Figure 2A).

Several candidate genes in this region were sequenced, including *At3g51460*, which was predicted to encode a Sac1p-like phosphoinositide phosphatase protein. The SAC domain of this protein, previously designated At SAC7 (Zhong and Ye, 2003), contains all seven of the conserved motifs of yeast Sac1p (Figure 2B). In sequencing the *rhd4-1* allele, a G→A base pair substitution was identified in *At3g51460* at the first base of the first intron, which would prevent proper intron splicing. A second

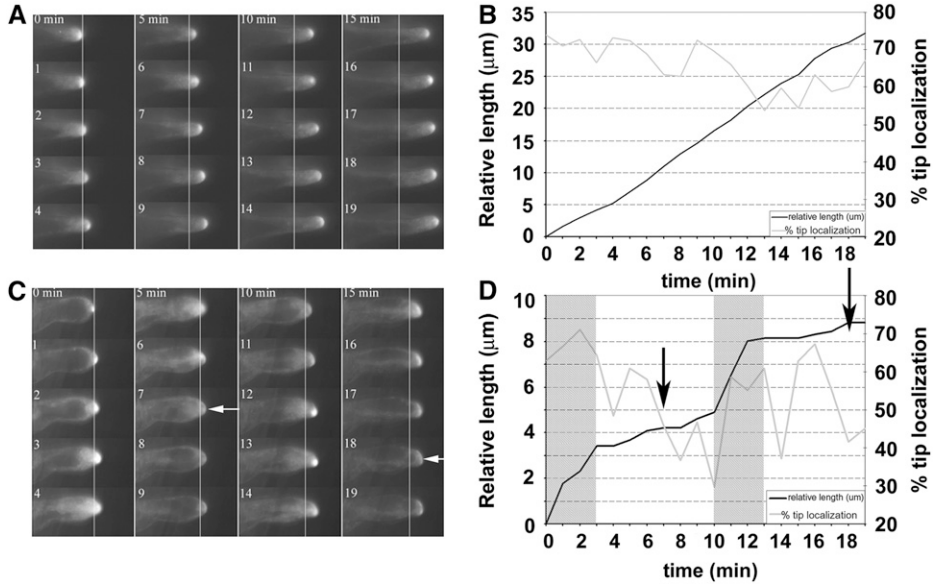

Figure 1. Spatial and Temporal Distribution of RabA4b Is Altered in *rhd4-1* Mutants.

Wild-type and *rhd4-1 Arabidopsis* seedlings expressing EYFP-RabA4b were visualized by time-lapse fluorescence microscopy, and frames from a 20-min period are shown, with a reference line for root hair length at time 0. Relative length was measured from time 0 as 0 μm. The fluorescent signal located within the proximal 7% of the length of the root hair was defined as tip fluorescence, and this was presented as a percentage of the fluorescence detected within the entire root hair.

(A) EYFP-RabA4b was localized to the tip of a growing wild-type root hair over a time period of 20 min.

(B) Quantification of EYFP-RabA4b localization in a wild-type root hair. Black line, relative length of the root hair in micrometers; gray line, percentage of tip localization of the fluorescent signal.

(C) EYFP-RabA4b localization is altered in a growing *rhd4-1* root hair. Arrows indicate time points at which the root hair is bulging, and EYFP-A4b localization is lost.

(D) Quantification of EYFP-RabA4b localization in an *rhd4-1* root hair. Root hair tip growth correlates with increased EYFP-RabA4b tip fluorescence (shaded regions). Arrows indicate time points at which the root hair is bulging, and EYFP-A4b localization is lost. Black line, relative length of the root hair in micrometers; gray line, percentage of tip localization of the fluorescent signal.

ethyl methanesulfonate (EMS)–generated *rhd4* allele, designated *rhd4-2*, contained a G449S amino acid substitution in motif VII of the SAC phosphatase domain (asterisk in Figure 2B). Similar mutations in this conserved region were previously isolated and shown to disrupt phosphatase activity in yeast Sac1p (Hughes et al., 2000). Therefore, both the *rhd4-1* and *rhd4-2* alleles contained mutations that would potentially inactivate the phosphoinositide phosphatase protein encoded by *At3g51460*.

To confirm the identification of *RHD4* as *At3g51460*, SALK T-DNA insertion lines were obtained (Alonso et al., 2003) and analyzed for mutant root hair phenotypes. Two homozygous lines were identified and were designated *rhd4-3* and *rhd4-4*, which have insertions located in the second and fourth introns, respectively (Figure 2A). RNA was isolated from seedlings of the wild type and all four *rhd4* alleles, and cDNA was amplified for RT-PCR. Transcript levels were significantly reduced in *rhd4-1*, *rhd4-3*, and *rhd4-4*, although low levels of transcript could be detected with increased PCR cycles (Figure 3A). As expected, *rhd4-2* transcript levels are similar to the wild type, as this allele simply contains a base pair substitution.

Since low levels of two differently sized transcripts were detected in the *rhd4-1* mutant, sequences were obtained for both to determine if any wild-type transcript was present. Both low-level transcripts were nonfunctional, with the larger transcript (Figure 3A, asterisk) containing the entire first intron due to the *rhd4-1* splicing mutation. The smaller transcript had an improperly spliced intron, and both transcripts resulted in premature stop codons (see Supplemental Figure 1 online). Therefore, all four of the *rhd4* alleles we characterized are either nonfunctional (*rhd4-1* and *rhd4-2*) or expression is virtually eliminated (*rhd4-3* and *rhd4-4*). All four alleles have the same phenotype of short, bulged, and branched root hairs (Figure 3B). Quantification of root hair length demonstrated that all four alleles have significantly shorter root hairs (Figure 3D), and all four alleles have a similar percentage of morphologically aberrant root hairs (Table 1).

Finally, genetic complementation was used to demonstrate that *At3g51460* was indeed the gene responsible for the *rhd4-1* mutation. We introduced wild-type *At3g51460* into the *rhd4-1* background using *Agrobacterium tumefaciens*–mediated transformation. Expression of wild-type *At3g51460* in the *rhd4-1* mutant background under the control of its own promoter resulted in fully expanded, morphologically wild-type root hairs (Figure 3C). Expression of an EYFP-At3g51460 fusion protein from its own promoter also rescued the *rhd4-1* mutant phenotype (Figure 3C). Quantification of root hair length demonstrated that both the cDNA-complemented line and the EYFP-cDNA–complemented

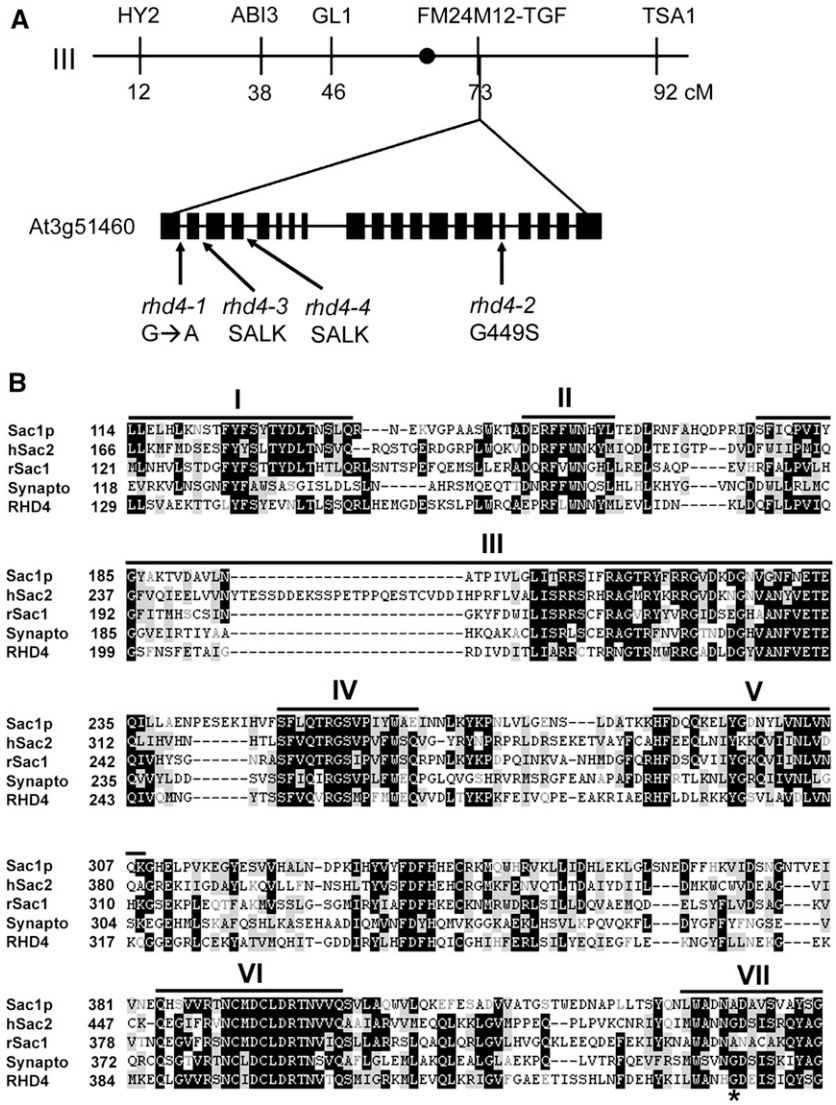

Figure 2. RHD4 Encodes a Sac1p-Like Phosphoinositide Phosphatase.

(A) Map-based cloning of the *rhd4* mutation. RHD4 is located on the right arm of chromosome 3, At3g51460. For spatial reference, described genetic markers are shown with their corresponding map position in centimorgans (cM). The *rhd4-1* allele had a G→A base pair substitution at the first base of the first intron. The *rhd4-2* allele had a mutation in exon 16 causing an amino acid substitution of Gly to Ser, G449S, in the protein. Two SALK T-DNA insertional lines were obtained, designated *rhd4-3* and *rhd4-4*, and these had insertions in the second and fourth introns, respectively.

(B) Amino acid alignment of the SAC domains of RHD4 and other SAC domain proteins from yeast and animals. The SAC domain sequences of yeast Sac1 (Sac1p), human Sac2 (hSAC2), rat SAC1 (rSAC1), human synaptojanin (Synapto), and RHD4 were aligned using ClustalW. Identical amino acids are shaded black, and similar amino acids are shaded gray. The seven conserved motifs of the SAC domain (Hughes et al., 2000) are marked by solid lines above the sequences. The location of the *rhd4-2* G449S amino acid substitution in motif VII is marked by an asterisk.

line have significantly longer root hairs than the uncomplemented *rhd4* alleles (Figure 3D), and both lines have root hairs with a restored wild-type morphology (Table 1).

RHD4 Is a PI(4)P Phosphatase

Based on sequence similarity, *RHD4* was predicted to encode a phosphoinositide phosphatase. To test this, we expressed and purified both wild-type RHD4 and the mutant *rhd4-2* N-terminal catalytic domains from *Escherichia coli* as glutathione *S*-transferase (GST) fusion proteins for an in vitro phosphatase activity assay. As RHD4 was most similar to the yeast Sac1p, which has been shown to have PI(4)P phosphatase activity (Hughes et al., 2000; Foti et al., 2001; Zhong and Ye, 2003), we first tested whether purified RHD4 had PI(4)P phosphatase activity. GST-RHD4 displayed higher levels of PI(4)P phosphatase activity than GST

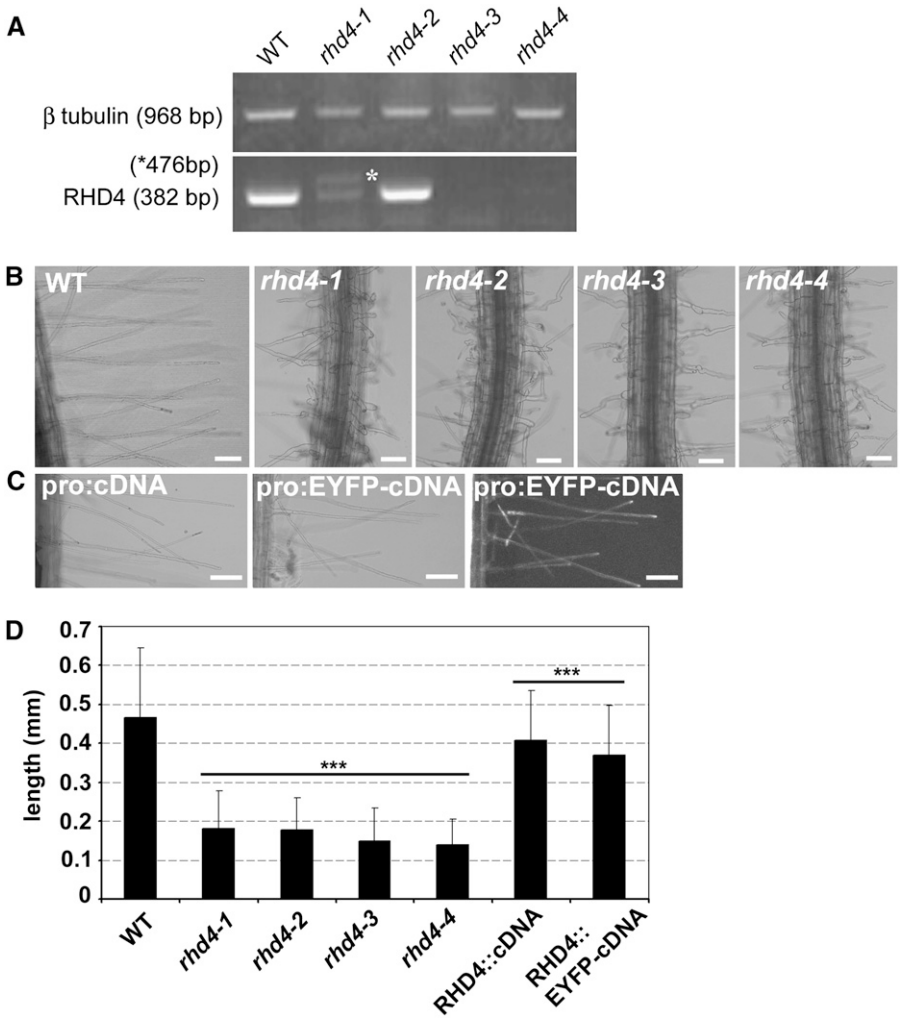

Figure 3. RHD4 Alleles and Complementation.

(A) RT-PCR of *RHD4* expression in wild-type seedlings and in mutant seedlings containing each of the different *rhd4* alleles. RNA was extracted from seedlings for cDNA synthesis and RT-PCR. In the *rhd4-1* sample, a larger band was observed (asterisk), and this band corresponds to the RHD4 transcript including the first intron due to the G→A base pair substitution, which prevents proper splicing. β-tubulin is used as an internal loading control.

(B) Phenotypes caused by the *rhd4* mutant alleles. Bars = 100 μm.

(C) Complementation of the *rhd4-1* mutation. *rhd4-1* mutant *Arabidopsis* plants were transformed by *Agrobacterium*-mediated transformation with an At3g51460 native promoter-At3g51460 cDNA construct (left panel) and a native promoter-EYFP-cDNA construct observed by light microscopy (middle panel) and fluorescence microscopy (right panel). Bars = 100 μm.

(D) Quantification of root hair length. Root hairs of wild-type, *rhd4* alleles, and complemented seedlings were measured ($n = 314$, 311, 272, 268, 308, 464, and 398 root hairs, respectively). Error bars represent 1 SD.

alone (Figure 4A). Additionally, the *rhd4-2* allele containing the G449S mutation in the phosphatase domain reduced the PI(4)P phosphatase activity to the residual levels observed for GST alone (Figure 4A). To determine if in vitro PI phosphatase activity detected for GST-RHD4 was specific for PI(4)P, we also tested whether RHD4 displayed phosphatase activity for other PI isoforms. While we did observe some limited phosphatase activity with different phosphoinositides, RHD4 had significantly higher phosphatase activity against PI(4)P (Figure 4B), consistent with this protein being a PI(4)P phosphatase.

While many PI phosphatases have been shown to demonstrate activity against a broad number of substrates in vitro, their in vivo activities may be quite different due to restricted access to substrates based on their subcellular localization (Hughes et al., 2000). Therefore, to confirm that RHD4 also had PI(4)P phosphatase activity in vivo, we assessed levels of phosphoinositides present in wild-type and *rhd4-1* mutant roots. Wild-type and *rhd4-1* seedlings were grown in the presence of ^{3}H-inositol, and phospholipids were extracted from root tissues for comparison by HPLC. In *rhd4-1* roots, PI(4)P levels were ~50% higher than

Table 1. Root Hair Morphology of *rhd4* Alleles and Complemented Lines

	Wild Type	Branched	Bulged	Popsicle	Wavy	Jagged
Wild type	94.27 ± 2.26	0.80 ± 0.81	1.88 ± 0.96	0.09 ± 0.26	0.29 ± 0.43	2.68 ± 1.95
rhd4-1	45.69 ± 8.56	5.35 ± 1.81	39.69 ± 8.11	0.85 ± 1.55	3.63 ± 3.55	4.79 ± 2.05
rhd4-2	55.59 ± 14.18	6.89 ± 4.27	30.55 ± 6.54	1.00 ± 1.10	1.04 ± 1.03	5.56 ± 6.17
rhd4-3	35.68 ± 14.00	8.49 ± 5.89	46.16 ± 6.31	0.00	1.34 ± 0.88	8.33 ± 3.72
rhd4-4	39.59 ± 8.89	7.01 ± 2.68	45.09 ± 10.48	0.75 ± 2.11	1.77 ± 1.15	5.79 ± 1.54
Complemented	85.07 ± 7.13	6.49 ± 2.71	4.08 ± 2.82	0.00	1.23 ± 1.53	3.12 ± 1.42
EYFP-complemented	90.89 ± 5.97	1.02 ± 0.73	1.45 ± 1.42	0.00	1.02 ± 0.73	5.62 ± 4.52

Percentages of each root hair class (defined in Preuss et al., 2006) were determined for the wild type, all four *rhd4* alleles, the native promoter-cDNA complemented line, and the native promoter-EYFP-cDNA complemented line (n = 1152, 1720, 1529, 1365, 1482, 983, and 947 root hairs, respectively). Errors represent the SD of the average for each line.

those in wild-type roots (Figures 4C and 4D). Based on these results, we concluded that RHD4 acts as a PI(4)P phosphatase in vivo and that loss of this activity in *rhd4* mutants results in overaccumulation of this phosphoinositide isoform.

PI(4)P Localization Is Altered in *rhd4-1* Root Hairs

Because RHD4 displayed PI(4)P phosphatase activity in vitro and in vivo, we were interested whether loss of this activity would result in altered accumulation or distribution of PI(4)P within developing root hairs. Therefore, we were interested in observing localization of PI(4)P pools in root hairs. We decided to create an EYFP biosensor that would bind to pools of PI(4)P in living plants. These types of PI binding biosensors have been widely used in mammalian systems (Varnai and Balla, 2007). We compared the in vivo binding of the well-characterized mammalian proteins FYVE and FAPP1. A tandem repeat of the FYVE domain (2XFYVE) has been used to visualize PI(3)P in mammalian cells (Gillooly et al., 2000) and in *Arabidopsis* root hairs, where PI(3)P has been localized to endosomal compartments (Voigt et al., 2005b). The PH domain of FAPP1 has been used to visualize PI(4)P in mammalian cells (Godi et al., 2004; Balla et al., 2005). In in vitro lipid binding assays, GST-2XFYVE showed specific binding to PI(3)P, and GST-FAPP1 showed specific binding to PI(4)P (Figure 5A). GST alone does not bind any of the lipids.

GFP-2XFYVE was localized to the endosomal compartment throughout wild-type root hairs (Figure 5B), and its distribution was unchanged in the *rhd4-1* background (Figure 5C), demonstrating that PI(3)P localization is not altered by mutation of the RHD4 phosphatase. In wild-type root hairs, EYFP-FAPP1 was localized primarily to the plasma membrane in the tips of growing root hairs (Figures 5D and 6A; see Supplemental Movie 3 online), although some internal membranes appeared to be lightly labeled by the EYFP-FAPP1 protein as well (Figure 5D, arrowheads). By contrast, in *rhd4-1* root hairs, EYFP-FAPP1 accumulated predominantly on internal membrane compartments within the tip. We observed little accumulation of EYFP-FAPP1 in the plasma membrane at the tips of root hair cells (Figures 5G and 6B; see Supplemental Movie 4 online).

To better demonstrate the difference between EYFP-FAPP1 localization in wild-type and *rhd4-1* root hairs, we studied the localization of the fusion protein in root hair cross sections. Cross sections at various positions within the root hair tip were obtained from z-stacks using Imaris software, and ImageJ was used to quantify the pixel intensity along a vertical line through the center of the cross section as described in Methods. In wild-type root hairs (Figure 5D), EYFP-FAPP1 was localized primarily to the plasma membrane, and in cross section and by quantification, the pixel intensity shows two peaks corresponding to the two edges of the root hair (Figures 5E and 5F). However, in *rhd4-1* root hairs, EYFP-FAPP1 was found on membrane compartments throughout the root hair (Figure 5H, arrowheads); therefore, in cross section and by quantification, the pixel intensity is variable (Figures 5H and 5I). We have observed FAPP1 localization in multiple transgenic *rhd4* lines and in lines where EYFP-FAPP1 was crossed into the *rhd4* background; all lines we observed show the same FAPP1 localization. These results strongly support the conclusion that mutation of the RHD4 PI(4)P phosphatase results in altered subcellular distribution of PI(4)P within the root hair cell, while distribution of PI(3)P remains unchanged.

The Actin Cytoskeleton Is Altered in *rhd4-1* Epidermal Cells

Yeast Sac1p mutants are known to have defects in actin cytoskeleton organization (Foti et al., 2001), and mutation of At *SAC1* also results in altered actin cytoskeleton organization in fiber and pith cells of elongating stems (Zhong et al., 2005). We were interested in determining whether mutation of the gene encoding the RHD4 phosphatase caused similar defects in actin organization. The GFP-FABD2 actin filament marker (Voigt et al., 2005a) was used to observe the actin cytoskeleton in wild-type and *rhd4-1* root hairs and epidermal cells. Actin filament organization does not appear to be altered in *rhd4-1* root hairs (Figures 7C and 7D) compared with wild-type root hairs (Figures 7A and 7B). However, in root epidermal cells, more actin patches were observed and filaments were thinner in *rhd4-1* cells (Figure 7F) compared with wild-type cells (Figure 7E).

RHD4 Colocalizes with RabA4b in the Tips of Root Hairs

The altered localization of PI(4)P observed on internal membranes in *rhd4-1* root hairs implied that wild-type RHD4 phosphatase activity limited the levels of this phosphoinositide in membranes of these internal compartments. It is known that yeast Sac1p is localized to both the endoplasmic reticulum (ER)

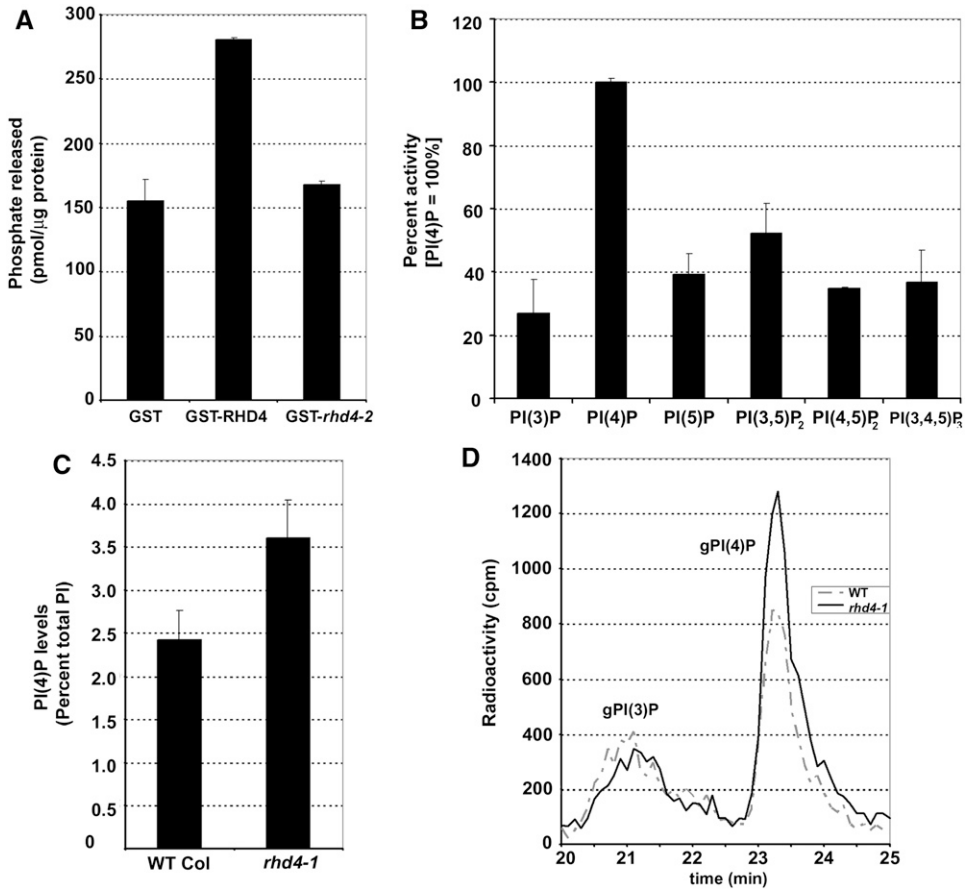

Figure 4. RHD4 Is a PI(4)P Phosphatase.

(A) GST-RHD4 has high levels of PI(4)P phosphatase activity in vitro. GST, GST-RHD4, and GST-*rhd4-2* were expressed and purified from *E. coli*. Error bars represent the SD of two biological replicates.

(B) GST-RHD4 has low levels of activity against all other phosphoinositide substrates tested. Values are calculated with PI(4)P activity as 100%. For each substrate, phosphatase release was measured for GST and GST-RHD4; the GST values were then subtracted from GST-RHD4 values to eliminate background. Error bars represent the SD of two replicates.

(C) *rhd4-1* roots accumulate PI(4)P. Two-week-old wild-type and *rhd4-1* seedlings were transferred to 0.25× Murashige and Skoog (MS) media supplemented with ^{3}H-myoinositol for 40 h. Radiolabeled phospholipids were isolated from root tissue, deacylated, and fractionated with HPLC. PI(4)P levels were calculated as a percentage of total PI. Error bars represent the SD from the average of nine samples.

(D) Representative traces from the HPLC of ^{3}H-labeled phospholipids from *rhd4-1* and wild-type roots. The glycerophosphoinositol peaks (gPI) for gPI(3)P and gPI(4)P are shown. *rhd4-1* (black line) has elevated levels of PI(4)P compared with the wild type (gray line), while PI(3)P levels are comparable between the wild type and *rhd4-1*.

and Golgi compartments (Konrad et al., 2002), and mammalian Sac1 is predominantly localized to the ER (Nemoto et al., 2000). We were therefore interested in determining RHD4 subcellular localization in plants, specifically within root hairs. An EYFP-RHD4 fusion protein was constructed and transformed into *Arabidopsis* under control of the native *RHD4* promoter. EYFP-RHD4 was functional, as it was capable of rescuing the *rhd4-1* mutant phenotype (Figures 3C and 3D, Table 1).

Intriguingly, subcellular EYFP-RHD4 was localized to the tips of growing root hairs (Figures 3C and 8A), showing a strikingly similar distribution to that observed for EYFP-RabA4b (Figure 8B). To compare the localization of RHD4 and RabA4b to Golgi and ER compartments, YFP-Golgi (G-yk) and YFP-ER (ER-yk) were obtained as markers for the Golgi and ER (Nelson et al., 2007). In root hairs, the tip-restricted localization pattern of RHD4 and RabA4b is distinct from YFP-Golgi (Figure 8C) and YFP-ER (Figure 8D), which are distributed throughout the cytoplasm of the root hair cell. Localization in root epidermal cells is also shown for EYFP-RabA4b (Figure 8E), YFP-Golgi (Figure 8F), and YFP-ER (Figure 8G). Some cells contain bright fusiform bodies that are local extensions of the ER (Nelson et al., 2007). However, EYFP-RHD4 is not expressed highly enough to image the localization in these cells; therefore, its epidermal cell localization could not be compared.

To further determine whether RHD4 and RabA4b were localized to the same compartment in root hairs, we observed the

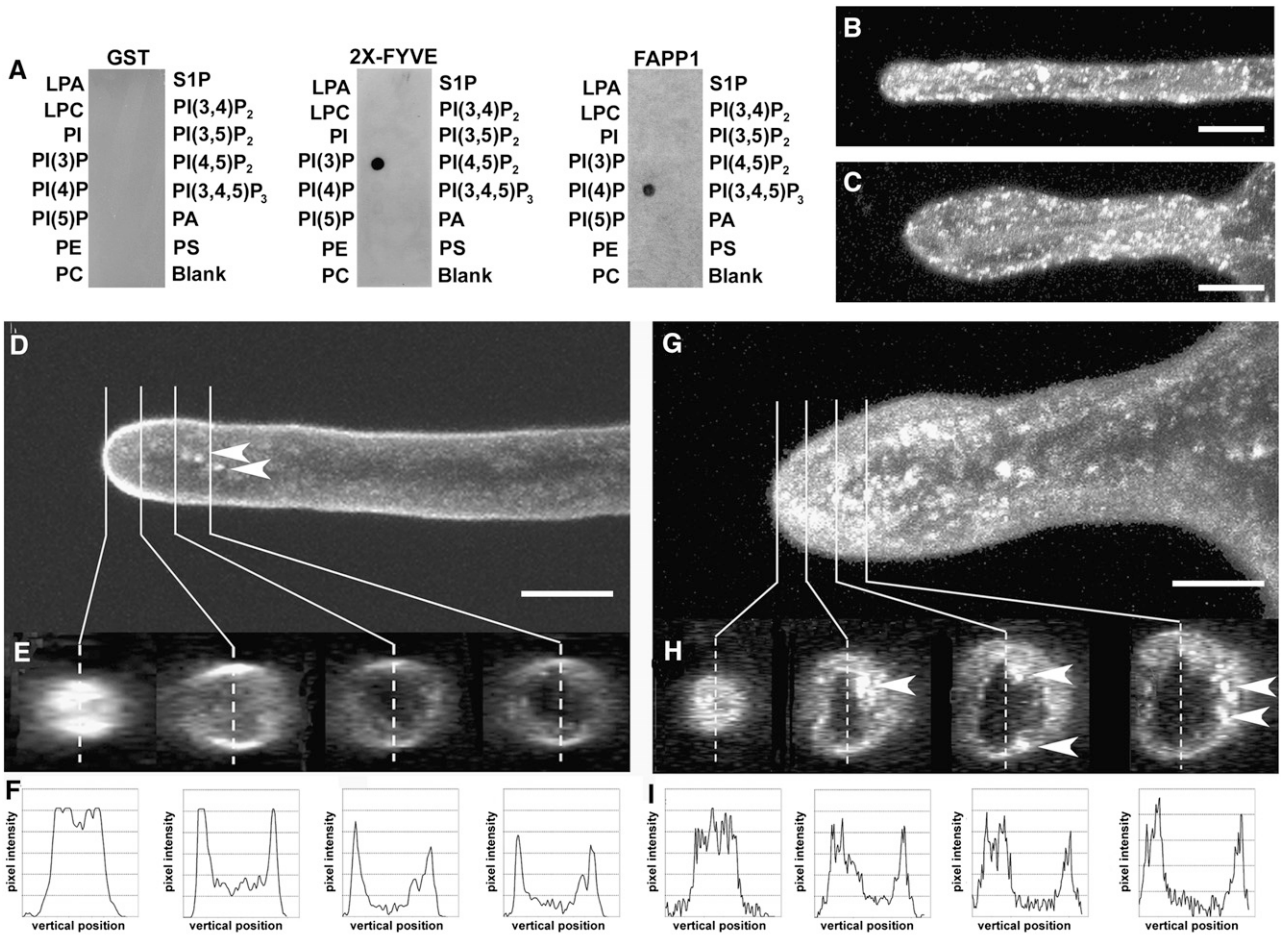

Figure 5. EYFP-FAPP1 Is Localized to Subcellular Membrane Compartments in *rhd4-1* Root Hairs.

(A) GST, GST-2XFYVE, and GST-FAPP1 lipid binding assays.
(B) GFP-FYVE, a PI(3)P binding protein, is localized to the endosomal compartment in wild-type root hairs. A z-stack projection is shown. Bar = 10 μm.
(C) GFP-FYVE localization in the *rhd4-1* background. A z-stack projection is shown. Bar = 10 μm.
(D) EYFP-FAPP1 is localized to the tips of growing wild-type root hairs. Arrowheads show localization to some subcellular membrane compartments. A z-stack projection of a wild-type root hair is shown. Bar = 10 μm.
(E) EYFP-FAPP1 is enriched on the plasma membrane of wild-type root hairs. Cross sections were made through the z-stack projection at various positions in the tip region as represented by solid white lines. Cross sections were then used to quantify the amounts of EYFP-FAPP1 along a line, represented by the dashed white line.
(F) Quantification of EYFP-FAPP in wild-type cross sections. ImageJ was used to quantify the pixel intensity of EYFP-FAPP1 along a vertical line through the center of each cross section (dashed white line in **[E]**). Each pixel intensity plot corresponds to the cross section above it in **(E)**.
(G) EYFP-FAPP1 is accumulated on subcellular membrane compartments in *rhd4-1* root hairs. A z-stack projection of a wild-type root hair is shown. Bar = 10 μm.
(H) EYFP-FAPP1 is found on subcellular membrane compartments throughout *rhd4-1* root hairs (arrowheads). Cross sections were made through the z-stack projection at various positions in the tip region as represented by solid white lines. Cross sections were then used to quantify the amounts of EYFP-FAPP1 along a line, represented by the dashed white line.
(I) Quantification of EYFP-FAPP1 in *rhd4-1* cross sections. ImageJ was used to quantify the pixel intensity of EYFP-FAPP1 along a vertical line through the center of each cross section (dashed white line in **[H]**). Each pixel intensity plot corresponds to the cross section above it in **(H)**.

localization of the anti-RabA4b antibody (Preuss et al., 2004) in fixed root hairs from transformed plants expressing EYFP-RHD4. These compartments colocalize at the tips of fixed root hairs (Figures 8H and 8I), and no tip-localized fluorescence was detected when anti-RabA4b antibodies were left out (Figure 8J). We have previously demonstrated that RabA4b labels budding profiles emerging from plant TGN compartments and post-Golgi vesicular structures (Preuss et al., 2006). Furthermore, both RabA4b and its effector protein, PI-4Kβ1, colocalize in the tips of root hair cells on membranes that are distinct from plant Golgi compartments. Based on these results, we concluded that, unlike in yeast and mammals, the Sac1p-like PI(4)P phosphatase

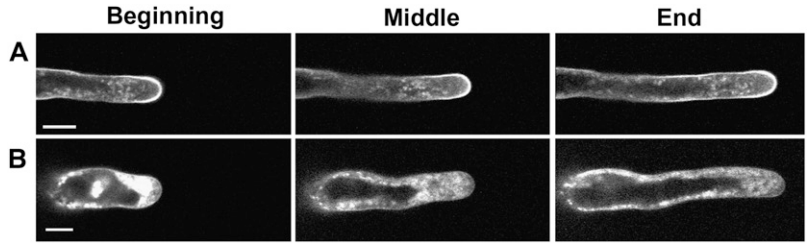

Figure 6. EYFP-FAPP1 Localization in Wild-Type and *rhd4-1* Root Hairs.

Arabidopsis seedlings expressing EYFP-FAPP1 were imaged by time-lapse fluorescence microscopy. Beginning, middle, and end frames are shown. Bars = 10 μm.
(A) Wild-type root hair. These frames are from Supplemental Movie 3 online.
(B) *rhd4-1* root hair. These frames are from Supplemental Movie 4 online.

localizes primarily to post-Golgi secretory compartments and participates in limiting the levels of PI(4)P in these membranes.

DISCUSSION

In *Arabidopsis*, polarized root hair growth is tightly associated with the polar accumulation of membrane compartments labeled by the RabA4b GTPase (Preuss et al., 2004). Furthermore, the RabA4b effector protein PI-4Kβ1 is required for proper control of polarized root hair expansion (Preuss et al., 2006). A number of root hair development mutants have been described with defects in root hair initiation and development. In this study, we further characterize one of these developmental mutants, *rhd4-1*, which displays shorter root hairs that sporadically form bulges as they expand (Schiefelbein and Somerville, 1990; Galway et al., 1999). In *rhd4-1* mutants, RabA4b-labeled compartments displayed altered distributions, with loss of tip localization that appeared to be associated with formation of root hair bulges (Preuss et al., 2004).

Here, we describe further analysis of the dynamics of EYFP-RabA4b localization in *rhd4-1* mutant root hairs and determine RHD4 to be a Sac1p-like phosphoinositide phosphatase. Furthermore, we have shown that RHD4 has PI(4)P phosphatase activity based on both in vitro and in vivo analyses. We found that

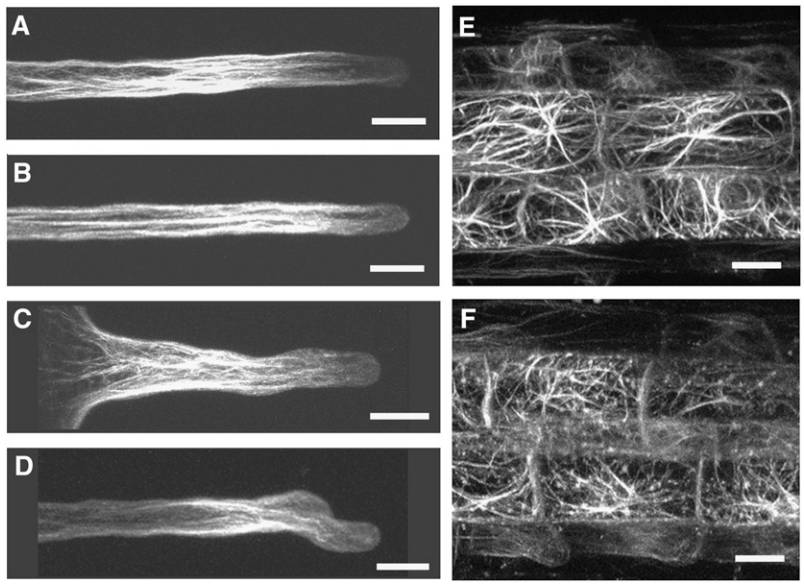

Figure 7. GFP-FABD2 Localization in *rhd4-1* Root Hairs and Epidermal Cells.

Arabidopsis seedlings expressing GFP-FABD2 (for localization of F-actin filament bundles) were imaged by confocal microscopy, and z-stack projections are shown. Bars = 20 μm.
(A) and **(B)** Localization in expanding wild-type root hairs. F-actin filament bundles are found throughout the root hair.
(C) and **(D)** Localization in expanding *rhd4-1* root hairs. F-actin filaments do not appear to be disturbed.
(E) Localization in wild-type root epidermal cells. A meshwork of F-actin is observed.
(F) Localization in *rhd4-1* root epidermal cells. A meshwork of F-actin is observed similar to the wild type; however, more actin patches are observed.

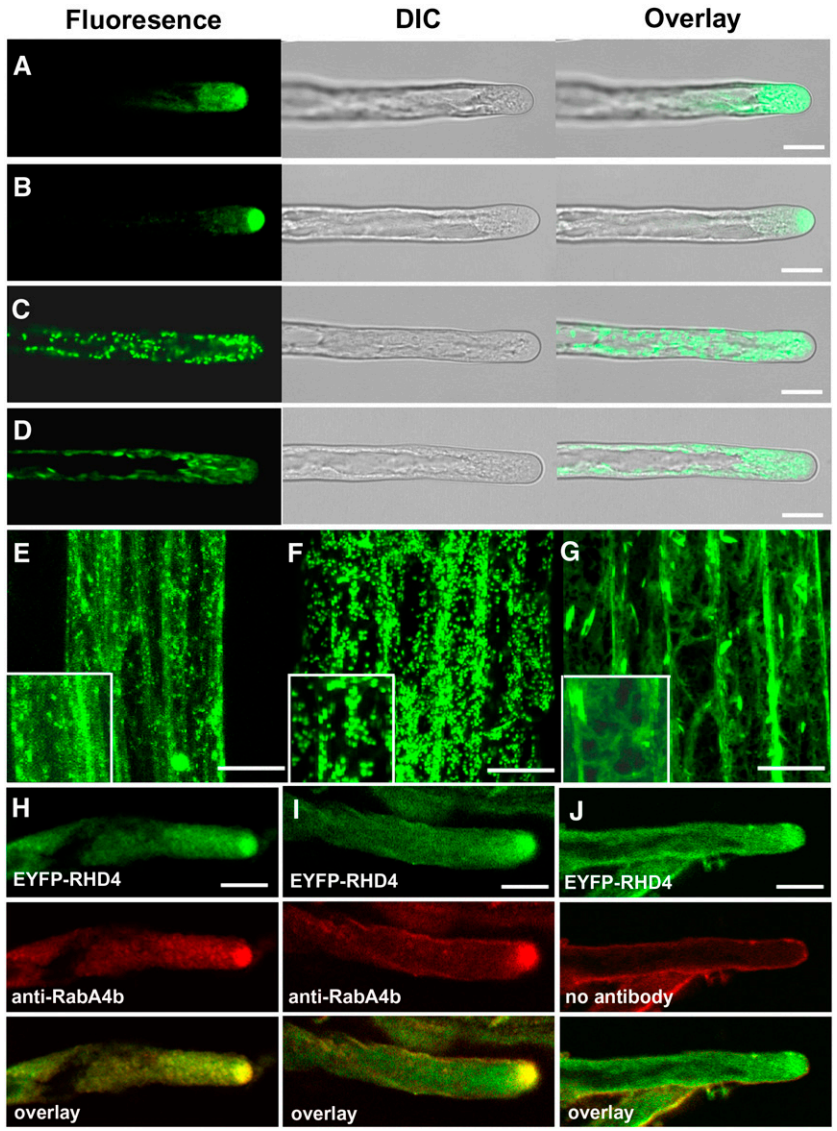

Figure 8. EYFP-RHD4 Is Localized to the Tips of Growing Root Hairs.

(A) to **(D)** *Arabidopsis* seedlings expressing various YFP fusion proteins were imaged by confocal microscopy. A medial fluorescence image, the corresponding differential interference contrast (DIC) image, and an overlay of these images are shown (columns, left to right). Bars = 10 μm.
(A) EYFP-RHD4 was expressed by its native promoter in *rhd4-1 Arabidopsis* plants and is localized to the tips of growing root hairs.
(B) EYFP-RabA4b is localized to a post-Golgi secretory compartment at the tips of growing root hairs.
(C) G-yk (a YFP-Golgi maker) is localized to the Golgi compartment throughout growing root hairs.
(D) ER-yk (a YFP-ER marker) is localized to the ER throughout growing root hairs.
(E) to **(G)** *Arabidopsis* seedlings expressing YFP fusion proteins were imaged by confocal microscopy. Inset: higher magnification. Z-stack projections are shown. Bars = 20 μm.
(E) EYFP-RabA4b localization in root epidermal cells.
(F) G-yk localization in root epidermal cells.
(G) ER-yk localization in root epidermal cells.
(H) to **(J)** *Arabidopsis* seedlings expressing EYFP-RHD4 were fixed, processed for immunolocalization of anti-RabA4b antibody, and analyzed by confocal microscopy. Medial sections are shown. Bars = 10 μm.
(H) and **(I)** RabA4b colocalizes with EYFP-RHD4 at the tips of root hairs. EYFP-RHD4 (green) and anti-RabA4b (red) are localized to overlapping tip-localized membrane compartments (yellow).
(J) Tip localization of anti-RabA4b is specific, as no tip-localized fluorescence was observed when anti-RabA4b primary antibody was left out.

PI(4)P was primarily associated with a tip-localized plasma membrane domain in wild-type plants, but this distribution was altered in *rhd4-1* mutant root hairs, accumulating significantly on internal membrane compartments. This qualitative difference may reflect the effect of increased amounts of PI(4)P in *rhd4-1* root tissues revealed by the in vivo labeling study. Also, RHD4 colocalized with RabA4b in a trans-Golgi network compartment at the tips of root hairs. These results, along with the previous determination that PI-4Kβ1 is required for proper control of root hair tip growth, demonstrate that regulation of PI(4)P levels plays a central role in polarized growth during root hair development.

Yeast SAC1 was initially characterized as a suppressor of a conditional-lethal temperature-sensitive actin mutation (Novick et al., 1989), and it was later identified as a phosphoinositide phosphatase (Hughes et al., 2000; Foti et al., 2001). Subsequently, Sac1p, an essential gene in yeast, has been shown to regulate PI(4)P levels and to play important roles in the Golgi apparatus, actin cytoskeleton dynamics, and other cellular functions (Hughes et al., 2000; Foti et al., 2001). Studies in *Drosophila melanogaster* have shown that mutation of Sac1 results in disruption of JNK mitogen-activated protein kinase signaling, resulting in embryo lethality (Wei et al., 2003). It is intriguing that, in plants, the *rhd4-1* null allele has defective root hairs but no other observed morphological defects. This may suggest that RHD4 phosphatase activity is particularly important in cells in which differentiation involves significant levels of polarized secretion, such as root hair cells.

One possible reason for the limited defects of a SAC phosphatase null mutant in *Arabidopsis* is that the genome contains nine SAC genes. Mutation of the RHD4 PI(4)P phosphatase results in aberrant root hair development, and no other phenotypes have been observed with this mutant, suggesting that its close family members SAC6 and 8 may have a redundant function in PI(4)P regulation in other parts of the plant. This may explain why, upon deletion of the RHD4 gene, we observed an approximate twofold increase in PI(4)P in *rhd4-1* mutant root tissue, as opposed to the 8- to 10-fold increase observed in yeast Sac1p mutants that contain only a single SAC1 gene (Guo et al., 1999; Hughes et al., 2000).

It is important to note that RHD4 is the only gene of this family (At SAC6, 7, and 8) expressed in root hairs, according to a promoter-GUS study (Despres et al., 2003), and this may explain why only a root hair phenotype is observed in *rhd4* mutants. When expressed under the control of its native promoter, EYFP-RHD4 is localized to the tips of root hairs and colocalized with EYFP-RabA4b, suggesting that RHD4 is also localized to this post-Golgi compartment. By contrast, in yeast, Sac1p has been localized to both ER and Golgi membranes (Konrad et al., 2002), while rat Sac1 was localized to the ER (Nemoto et al., 2000).

Previously, Despres et al. (2003) found RHD4 was colocalized to the ER when a C-terminal GFP fusion of the protein was expressed in tobacco (*Nicotiana tabacum*) BY2 cells. However, it is possible that overexpression of this integral membrane protein caused mislocalization or that BY2 cells are an inappropriate tissue for observing the localization of this fusion protein. Alternatively, perhaps this C-terminal GFP fusion could not be trafficked properly, whereas our N-terminal EYFP fusion is known to be functional, as demonstrated by complementation of the *rhd4-1* phenotype. It also is possible that, in cells undergoing high levels of polarized secretion such as root hairs and pollen tubes, RHD4 is found in subcellular locations unique from their yeast or mammalian homologs to specifically influence membrane trafficking required for polarized secretion.

Earlier transmission electron microscopy studies found that *rhd4-1* root hairs had localized cell wall thickenings that were thought to form during root hair bulging (Galway et al., 1999). These thickenings could occur in *rhd4-1* root hairs when an overaccumulation of PI(4)P leads to increased vesicle production and/or spurious fusion at the tips of root hairs, resulting in increased delivery of cell wall materials and in root hair bulging. Interestingly, in yeast, loss of Sac1p leads to increased trafficking of chitin synthase to the plasma membrane, and Sac1p has been identified as an antagonist of Pik1p, the yeast homolog of PI-4Kβ1 (Schorr et al., 2001). In plants, loss of PI-4Kβ activity results in compromised control of root hair tip growth (Preuss et al., 2006), as does the loss of RHD4 PI(4)P phosphatase activity.

Taken together, we propose that the defect in proper root hair tip growth upon mutation of either of these components is due to loss of proper regulation of PI(4)P levels within these cells. We found that EYFP-RHD4 was localized to subcellular compartments in the tips of root hairs (Figure 8), where we propose it functions to regulate levels of PI-4Kβ1-generated PI(4)P, and that it normally restricts the levels of PI(4)P to vesicles at the extreme tips of growing root hairs. In the *rhd4-1* mutant, loss of the phosphatase activity would result in release of this inhibition, and PI(4)P accumulation on these subcellular membranes could occur (Figures 5G). This may cause an increased accumulation of PI(4)P-labeled vesicles, resulting in wider root hairs, and in extreme cases bulge formation may occur.

Our results are similar to results for PLC3 regulation of $PI(4,5)P_2$ in pollen tubes in which PLC3 is targeted to the flanks of pollen tube tips, but not to the apex, where it functions to prevent overaccumulation of $PI(4,5)P_2$ outside of the apex, thus maintaining $PI(4,5)P_2$ at the tips (Helling et al., 2006). Also of interest is a recent study in animal cells demonstrating that enrichment of $PI(4,5)P_2$ on the apical plasma membrane of epithelial cells is due to the localization of the $PI(3,4,5)P_3$ phosphatase PTEN (Phosphatase and Tensin homolog on chromosome 10) to this subcellular domain (Martin-Belmonte et al., 2007). This study suggests that $PI(4,5)P_2$ acts as a signal to differentiate the apical membranes from basolateral membranes in these cells, a process that had not previously been understood.

Additionally, Nishio et al. (2007) have recently found that SHIP1, a $PI(3,4,5)P_3$ phosphatase, functions to regulate the localized accumulation of $PI(3,4,5)P_3$ required for polarization and motility in mouse neutrophils. These observations and the results we present here demonstrate that phosphoinositide signals have an effect on cellular morphogenesis. Therefore, regulating not only the levels but also the locations where various phosphoinositides accumulate within cells during development may be a conserved mechanism to generate spatial cues that influence the establishment and maintenance of polarity.

In conclusion, we demonstrated that *RHD4* encodes a Sac1p-like phosphoinositide phosphatase that regulates a pool of PI(4)P, which ultimately influences root hair development. We found that both PI-4Kβ1 and RHD4 were localized to

RabA4b-labeled membranes in the tips of root hairs, where we propose that they function to maintain PI(4)P levels required for proper polarized secretion.

METHODS

Visualization of EYFP-RabA4b Localization

Wild-type and *rhd4-1 Arabidopsis thaliana* seedlings expressing EYFP-RabA4b were grown on 0.25× MS medium + 0.3% phytagel. Seven- to 10-d-old seedlings were transferred to a slide chamber through which media were exchanged by peristaltic pump, as previously described (Preuss et al., 2004). EYFP fluorescence was observed with a Nikon Eclipse E600 microscope with a ×40 Plan Apo lens (numerical aperture 1.2) with frames collected every 30 s. Relative length was defined as the change in root hair length from time 0 and length 0 μm. The fluorescent signal located within the proximal 7% of the length of the root hair was defined as tip fluorescence, and this was presented as a percentage of the total fluorescence detected within the entire root hair.

Map-Based Cloning

The *rhd4-1* mutant (Columbia ecotype) was crossed with *Arabidopsis* ecotype Landsberg *erecta* to generate F2 mapping plants. Coarse mapping was done with publicly available CAPS and SSLP genetic markers. Fine mapping of *rhd4-1* was done with CAPS and SSLP markers developed based on Landsberg sequence information from the Cereon *Arabidopsis* database (Jander et al., 2002).

For *rhd4-1* complementation, the pEarleyGate302 vector (Earley et al., 2006) was used. The wild-type RHD4 cDNA was generated by RT-PCR from wild-type Columbia cDNA template using the primers *Xba*I RHD4 forward (5′-TCTAGAATGGAGACGGTTGATTCTCGG-3′) and *Pac*I RHD4 reverse (5′-TTAATTAATCAGCCTCTGGGCTTGTG-3′) and inserted into pEarleyGate302 using restriction sites for *Xba*I and *Pac*I. The RHD4 upstream sequence was cloned using the primers RHD4 Gateway promoter forward (5′-CACCAATATTATGTTTTCACAAATAAGGAAAGTTTCC-3′) and RHD4 Gateway promoter reverse (5′-ACTAAAATCAAACAAGAGACAAAAGAAGATTC-3′) and was recombined by Clonase reaction into pEarleyGate302.

rhd4-1 plants were transformed with *Agrobacterium tumefaciens* by the floral dip method (Clough and Bent, 1998). Transgenic plants were selected on 0.25× MS + Basta (glufosinate ammonium; Fisher) and carried to the T2 generation to verify complementation of the *rhd4-1* phenotype.

Characterization of Additional RHD4 Alleles

The *rhd4-2* EMS allele was obtained from J. Schiefelbein (University of Michigan, Ann Arbor, MI). The RHD4 insertion mutants were obtained from the SALK T-DNA collection (*rhd4-3* is SALK_079231 and *rhd4-4* is SALK_092575; ABRC) (Alonso et al., 2003). Wild-type and mutant seedlings were grown in 0.25× MS + 0.3% phytagel, transferred to a slide, and imaged using a Nikon Eclipse E600 microscope with a ×40 Plan Apo lens (numerical aperture 1.2). The T-DNA insertion site in each line was confirmed by sequencing (primers LBA1 5′-TGGTTCACGTAGTGGGCCATCG-3′, *rhd4-3* 5′-GATCCAACACGTTCACTCTCAG-3′, and *rhd4-4* 5′-TCCATGAAGCTCATCGGTTG-3′). Root hair length was quantified by measuring root hairs with Image J and calculating the average and standard deviation. Significance was determined using a two-sample *t* test assuming unequal variances.

RT-PCR

Wild-type Columbia *Arabidopsis* seedlings were grown at 22°C with 16 h of light for 10 d. Total RNA was extracted using the RNeasy kit (Qiagen), and cDNA was made according to TITANIUM one-step RT-PCR kit instructions (Clontech) with the primers RHD4 RT forward (5′-TCTAGAATGGAGACGGTTGATTCTCGG-3′) and RHD4 RT reverse (5′-TGGAGAACTCGGTCTCCATC-3′). Generation of β-tubulin cDNA from the same template RNA was used to equalize levels of cDNA (β-tubulin forward 5′-CCTGATAACTTCGTCTTTGG-3′ and β-tubulin reverse 5′-GTGAACTCCATCTCGTCCAT-3′). The amplification program consisted of 30 s at 94°C, 30 s at 65°C, and 1 min at 68°C for 35 cycles, followed by a 2-min extension at 68°C.

Protein Purification

Truncated cDNAs of *RHD4* and the *rhd4-2* allele of *RHD4* (lacking the C-terminal transmembrane domains) were generated by RT-PCR for expression as GST fusion proteins with primers *Sma*I GST-RHD4 forward (5′-CCCGGGGATGGAGACGGTTGATTCTCGG-3′) and *Xho*I GST-RHD4 truncated reverse (5′-CTCGAGTCACCCTTGCAAGAGATCAATTGC-3′). These cDNAs were then inserted in frame into the pGEX-4T1 expression vector using restriction sites for *Sma*I and *Xho*I. The fusion proteins were expressed in *Escherichia coli* Rosetta cells and purified with glutathione sepharose beads. Purified protein was eluted with 50 mM Tris-HCl, pH 7.5, 100 mM NaCl, 15 mM glutathione, 2 mM DTT, and 0.25% β-D-octylglucoside.

The cDNA encoding the 2XFYVE PH domain was generated using pGFP-2XFYVE as a template, with primers *Bam*HI GST-FYVE forward (5′-GGATCCGAAAGTGATGCCATGTTC-3′) and *Xho*I GST-FYVE reverse (5′-GAGCTCTGCCTTCTTGTTCAGCTG-3′). The cDNA encoding the FAPP1 PH domain was generated using pHAN-hFAPP1 (gift from Marino Zerial) as a template, with primers *Nde*I GST-FAPP1 forward (5′-GGGAATTCCATATGATGGAGGGGGTGTTGTAC-3′) and *Kpn*I GST-FAPP1 reverse (5′-GGGGTACCTCAAGTCCTTGTATCAGTCAAACATGC-3′). These cDNAs were then inserted in frame into the pET41 expression vector with the restriction sites *Bam*HI and *Xho*I (2XFYVE) and *Nde*I and *Kpn*I (FAPP1). The fusion proteins, along with the pET41 GST control, were expressed in *E. coli* Rosetta cells (GST-FAPP1 and GST) or BL21 cells (GST-2XFYVE) and purified with glutathione sepharose beads. Purified protein was eluted with 50 mM Tris, pH 8.0, 100 mM NaCl, 15 mM glutathione, and 5 mM β-mercaptoethanol.

Phosphatase Activity Assay

Purified recombinant GST, GST-RHD4, and GST-*rhd4-2* were used for a phosphoinositide phosphatase activity assay. diC16 phospholipid substrates (Echelon) were dissolved in 1:2:0.8 $CHCl_3$:MeOH:H_2O with the aid of sonication. The phosphatase activity of recombinant proteins was measured by mixing 2.5 μg of protein in reaction buffer (50 mM Tris-HCl, pH 7.5, 5 mM $MgCl_2$, 10 mM KCl, 100 mM NaCl, 0.25% β-D-octylglucoside, and 1 mM phenylmethylsulfonyl fluoride) with 100 μM phospholipid substrates in a 50-μL reaction volume and incubated at 30°C for 50 min, agitating every 10 min. The reactions were stopped by the addition of 100 μL Biomol Green (Biomol International), incubated at room temperature for 30 min, and the free phosphate released from the substrates was measured at OD_{620} and determined by comparison to $NaPO_4$ standards.

In Vivo Labeling of Phosphoinositides

Wild-type and *rhd4-1* mutant *Arabidopsis* seedlings were grown in 0.25× MS containing 10 μM reduced *myo*-inositol for 2 weeks. Two-week-old plants were radiolabeled with *myo*-2-[^{3}H] inositol at a concentration of 50 μCi/mL. Labeling was done in 1 mL in wells of a 24-well plate for 40 h on a gyratory shaker at 22°C.

Lipids were extracted using the protocol of Hama et al. (2000). Briefly, shoot and root tissues were separated, and root tissues were fixed in 5% trichloroacetic acid and incubated on ice for 1 h. Tissue was washed five

times with 10 mL of water, suspended in 0.5 mL of water in a tissue grinder, and homogenized with the addition of 0.75 mL 95% ethanol: diethyl ether:pyridine (15:5:1 [v/v]). The homogenate was incubated at 57°C for 30 min. Cell debris was removed by centrifugation, and the supernatant was dried under N_2.

Dried lipids were resuspended in 2 mL of water:methylamine (3:7, methylamine is 40% [v/v] in ethanol) by water bath sonication and vortex, incubated for 50 min at 53°C, and dried under N_2. Deacylated lipids were suspended in 0.5 mL of water by water bath sonication and extracted with 1 mL of water-saturated *n*-butanol:petroleum ether:ethyl formate (20:4:1) four times. The aqueous phase was dried under N_2.

Deacylated lipids were analyzed by anion exchange HPLC as previously described (Bonangelino et al., 2002).

Lipid Binding Assays

Lipid binding assays were performed using PIP Strips (Echelon). PIP strips were blocked in 1× TBS, 0.1% Tween 20, and 5% fatty acid free BSA and then incubated with 1 nM protein at 4°C overnight (either GST, GST-FAPP, or GST-2XFYVE). Next, the PIP strips were washed with 1× TBS + 0.1% Tween 20, incubated with anti-GST antibody (1:2000 in blocking solution) for 1 h at room temperature, washed with 1× TBS + 0.1% Tween 20, and then incubated with anti-rabbit HRP secondary antibody (1:2500) for 1 h at room temperature. Finally, the PIP strips were washed with 1× TBS + 0.1% Tween 20 before developing with enhanced chemiluminescent reagent.

Localization of PI Pools

pCAMBIA-35S-EYFP-FAPP1 vectors were constructed by subcloning the EYFP-FAPP1 fusion from the vector pMON999YFP-PHFAPP into pCAMBIA (CAMBIA) using restriction sites *Nco*I and *Bam*HI. Wild-type and *rhd4-1* transgenic EYFP-FAPP1 plants were generated with *Agrobacterium* by the floral dip method (Clough and Bent, 1998).

Wild-type and *rhd4-1* EYFP-FAPP1 seedlings were observed on a confocal microscope (Zeiss LSM 510) with a ×40 Apochromat lens (numerical aperture 1.2). Z-stack sections of root hairs were taken, and three-dimensional projections from these stacks were used for the final images. For Figure 5D, there are 25 slices, taken 0.66 μm apart; for Figure 5G, there are 38 slices, taken 0.66 μm apart. Imaris software (Bitplane) was used to obtain cross sections of root hairs from the z-stacks. ImageJ (software developed by the National Institutes of Health and available from http://rsb.info.nih.gov/ij) was used to quantify the pixel intensity in the root hair cross sections.

GFP-2XFYVE *Arabidopsis* seed was a gift from F. Baluska (University of Bonn, Bonn, Germany). Seedlings were observed on a confocal microscope (Leica confocal system TCS SP2) with a ×63 Plan Apo lens (numerical aperture 1.2). Z-stacks of root hairs were taken, and three-dimensional projections from these stacks were used for the final images. For Figure 5B, there are 12 slices, taken 1.0 μm apart; for Figure 5C, there are 22 slices, taken μm apart.

Localization of EYFP-RHD4 and GFP-FABD2

The *RHD4* cDNA was generated by RT-PCR from wild-type Columbia cDNA using the primers RHD4 forward (5′-GTCGACATGGAGACGGTTGATTCTC-3′) and RHD4 reverse (5′-TCTAGATCAGCCTCTGGGCTTGTG-3′) and inserted into the pCAMBIA vector (CAMBIA) using restriction sites for *Sal*I and *Xba*I. The *RHD4* upstream sequence was generated by PCR from wild-type Columbia genomic DNA using the primers *Eco*RI RHD4 promoter forward (5′-GAATTCAATATTATGTTTTCACAAATAAGGAAAGTTTCC-3′) and *Nco*I RHD4 promoter reverse (5′-CCATGGACTAAAATCAAACAAGAGACAAAAGAAGATTC-3′). This sequence was inserted into pCAMBIA using restriction sites for *Eco*RI and *Nco*I to drive expression of EYFP-RHD4. Wild-type and *rhd4-1* EYFP-RHD4 plants were generated with *Agrobacterium* by the floral dip method (Clough and Bent, 1998).

G-yk and ER-yk *Arabidopsis* were a gift from A. Nebenfuhr (University of Tennessee, Knoxville, TN).

GFP-FABD2 *Arabidopsis* seed were a gift from F. Baluska (University of Bonn, Bonn, Germany). Pollen from wild-type GFP-FABD2 plants was crossed to *rhd4-1* stigmas to create *rhd4-1* GFP-FABD2 plants.

Seedlings were grown on 0.25× MS + 0.3% phytagel, and 7- to 10-d-old seedlings were observed on a confocal microscope (Zeiss LSM 510) with a ×40 Apochromat lens (numerical aperture 1.2). For images in Figure 7 and epidermal cell images in Figure 8, z-stacks of root hairs and epidermal cells were taken and three-dimensional projections were used for the final images. For Figure 7A, 25 slices were imaged; for Figure 7B, 22 slices; for Figure 7C, 25 slices; for Figure 7D, 38 slices; for Figure 7E, 47 slices; for Figure 7F, 43 slices. All slices were taken 1.06 μm apart. For Figure 8E, 26 slices were imaged; for Figure 8F, 22 slices; for Figure 8G, 10 slices. All slices were taken 1.0 μm apart. For root hair images in Figure 8, medial sections are shown.

Immunolocalization

EYFP-RHD4 *Arabidopsis* seedlings were processed for immunolocalization as previously described (Preuss et al., 2006). Primary anti-RabA4b antibody (Preuss et al., 2004) was used at a concentration of 1:100, and secondary anti-rabbit Cy3 was used at a concentration of 1:200. After primary and secondary antibody incubations, slides were mounted with Mowiol (Calbiochem). Samples were observed on a confocal microscope (Zeiss LSM 510) with a ×40 Apochromat lens (numerical aperture 1.2). Medial sections were used for the final images. Images were taken at the same laser power for accurate comparison of Cy3 signal.

Accession Numbers

The *RHD4/SAC7* Arabidopsis Genome Initiative number is *At3g51460*, and the GenBank accession number is AY227250. Accession numbers for the mutant alleles of *rhd4* shown in Figures 2A and 3B are as follows: The Arabidopsis Information Resource accession 1945311 or Germplasma CS2261 (*rhd4-1*), Germplasma CS16302 (*rhd4-2*), SALK_079231 (*rhd4-3*), and SALK_092575 (*rhd4-4*). The GenBank accession numbers for the sequences shown in Figure 2B are X51672 (Sac1p), NM_014937 (hSac2), NM_053798 (rSac1), and NM_003895 (Synaptojanin I).

Supplemental Data

The following materials are available in the online version of this article.

Supplemental Figure 1. *rhd4-1* Mutant Transcript Sequence.

Supplemental Movie 1. EYFP-RabA4b Is Localized to the Tips of Wild-Type Root Hairs.

Supplemental Movie 2. EYFP-RabA4b Localization Is Altered in *rhd4-1* Root Hairs.

Supplemental Movie 3. EYFP-FAPP1 Is Localized to the Plasma Membrane at the Tips of Wild-Type Root Hairs.

Supplemental Movie 4. EYFP-FAPP1 Localization Is Altered in *rhd4-1* Root Hairs.

Supplemental Movie Legends.

ACKNOWLEDGMENTS

We thank John Schiefelbein for sharing additional *rhd4* EMS mutant lines (*rhd4-2*), Frantisek Baluska for sharing GFP-2XFYVE and

GFP-FABD2 transformed *Arabidopsis* lines and the pGFP-2XFYVE plasmid, Andreas Nebenfuhr for sharing ER-yk and G-yk transformed *Arabidopsis* lines, Marino Zerial for the pHAN-hFAPP plasmid, Jonathan Markham for technical assistance with lipid extraction techniques, Amy Steward and Heather Bonner for technical assistance with FAPP1 work, and Howard Berg for help with various microscopy work. We thank Ralph Quatrano and his lab for bench space, reagents, and valuable discussion. We also thank Lois Weisman for technical help and input regarding in vivo analysis of PI-4P levels. This work was supported by the Department of Energy (DE-FG02-03ER15412 to E.N.).

Received July 17, 2007; revised December 17, 2007; accepted January 29, 2008; published February 15, 2008.

REFERENCES

Alonso, J.M., et al. (2003). Genome-wide insertional mutagenesis of *Arabidopsis thaliana.* Science **301:** 653–657.

Balla, A., Tuymetova, G., Tsiomenko, A., Varnai, P., and Balla, T. (2005). A plasma membrane pool of phosphatidylinositol 4-phosphate is generated by phosphatidylinositol 4-kinase type-III alpha: studies with the PH domains of the oxysterol binding protein and FAPP1. Mol. Biol. Cell **16:** 1282–1295.

Bankaitis, V.A., and Morris, A.J. (2003). Lipids and the exocytotic machinery of eukaryotic cells. Curr. Opin. Cell Biol. **15:** 389–395.

Bohme, K., Li, Y., Charlot, F., Grierson, C., Marrocco, K., Okada, K., Laloue, M., and Nogue, F. (2004). The Arabidopsis COW1 gene encodes a phosphatidylinositol transfer protein essential for root hair tip growth. Plant J. **40:** 686–698.

Bonangelino, C.J., Nau, J.J., Duex, J.E., Brinkman, M., Wurmser, A.E., Gary, J.D., Emr, S.D., and Weisman, L.S. (2002). Osmotic stress-induced increase of phosphatidylinositol 3,5-bisphosphate requires Vac14p, an activator of the lipid kinase Fab1p. J. Cell Biol. **156:** 1015–1028.

Clough, S.J., and Bent, A.F. (1998). Floral dip: A simplified method for Agrobacterium-mediated transformation of *Arabidopsis thaliana.* Plant J. **16:** 735–743.

de Graaf, P., Zwart, W.T., van Dijken, R.A., Deneka, M., Schulz, T.K., Geijsen, N., Coffer, P.J., Gadella, B.M., Verkleij, A.J., van der Sluijs, P., and van Bergen en Henegouwen, P.M. (2004). Phosphatidylinositol 4-kinasebeta is critical for functional association of rab11 with the Golgi complex. Mol. Biol. Cell **15:** 2038–2047.

De Matteis, M.A., and Godi, A. (2004). PI-loting membrane traffic. Nat. Cell Biol. **6:** 487–492.

Despres, B., Bouissonnie, F., Wu, H.J., Gomord, V., Guilleminot, J., Grellet, F., Berger, F., Delseny, M., and Devic, M. (2003). Three SAC1-like genes show overlapping patterns of expression in Arabidopsis but are remarkably silent during embryo development. Plant J. **34:** 293–306.

Di Paolo, G., and De Camilli, P. (2006). Phosphoinositides in cell regulation and membrane dynamics. Nature **443:** 651–657.

Dolan, L. (2001). How and where to build a root hair. Curr. Opin. Plant Biol. **4:** 550–554.

Dowd, P.E., Coursol, S., Skirpan, A.L., Kao, T.H., and Gilroy, S. (2006). Petunia phospholipase c1 is involved in pollen tube growth. Plant Cell **18:** 1438–1453.

Earley, K.W., Haag, J.R., Pontes, O., Opper, K., Juehne, T., Song, K., and Pikaard, C.S. (2006). Gateway-compatible vectors for plant functional genomics and proteomics. Plant J. **45:** 616–629.

Fischer, U., Men, S., and Grebe, M. (2004). Lipid function in plant cell polarity. Curr. Opin. Plant Biol. **7:** 670–676.

Foti, M., Audhya, A., and Emr, S.D. (2001). Sac1 lipid phosphatase and Stt4 phosphatidylinositol 4-kinase regulate a pool of phosphatidylinositol 4-phosphate that functions in the control of the actin cytoskeleton and vacuole morphology. Mol. Biol. Cell **12:** 2396–2411.

Galway, M.E., Lane, D.C., and Schiefelbein, J.W. (1999). Defective control of growth rate and cell diameter in tip-growing root hairs of the *rhd4* mutant of *Arabidopsis thaliana.* Can. J. Bot. **77:** 494–507.

Gillooly, D.J., Morrow, I.C., Lindsay, M., Gould, R., Bryant, N.J., Gaullier, J.M., Parton, R.G., and Stenmark, H. (2000). Localization of phosphatidylinositol 3-phosphate in yeast and mammalian cells. EMBO J. **19:** 4577–4588.

Godi, A., Di Campli, A., Konstantakopoulos, A., Di Tullio, G., Alessi, D.R., Kular, G.S., Daniele, T., Marra, P., Lucocq, J.M., and De Matteis, M.A. (2004). FAPPs control Golgi-to-cell-surface membrane traffic by binding to ARF and PtdIns(4). Nat. Cell Biol. **6:** 393–404.

Guo, S., Stolz, L.E., Lemrow, S.M., and York, J.D. (1999). SAC1-like domains of yeast SAC1, INP52, and INP53 and of human synaptojanin encode polyphosphoinositide phosphatases. J. Biol. Chem. **274:** 12990–12995.

Hama, H., Takemoto, J.Y., and DeWald, D.B. (2000). Analysis of phosphoinositides in protein trafficking. Methods **20:** 465–473.

Helling, D., Possart, A., Cottier, S., Klahre, U., and Kost, B. (2006). Pollen tube tip growth depends on plasma membrane polarization mediated by tobacco PLC3 activity and endocytic membrane recycling. Plant Cell **18:** 3519–3534.

Hughes, W.E., Cooke, F.T., and Parker, P.J. (2000). Sac phosphatase domain proteins. Biochem. J. **350:** 337–352.

Jander, G., Norris, S.R., Rounsley, S.D., Bush, D.F., Levin, I.M., and Last, R.L. (2002). Arabidopsis map-based cloning in the post-genome era. Plant Physiol. **129:** 440–450.

Konrad, G., Schlecker, T., Faulhammer, F., and Mayinger, P. (2002). Retention of the yeast Sac1p phosphatase in the endoplasmic reticulum causes distinct changes in cellular phosphoinositide levels and stimulates microsomal ATP transport. J. Biol. Chem. **277:** 10547–10554.

Kost, B., Lemichez, E., Spielhofer, P., Hong, Y., Tolias, K., Carpenter, C., and Chua, N.H. (1999). Rac homologues and compartmentalized phosphatidylinositol 4,5-bisphosphate act in a common pathway to regulate polar pollen tube growth. J. Cell Biol. **145:** 317–330.

Martin-Belmonte, F., Gassama, A., Datta, A., Yu, W., Rescher, U., Gerke, V., and Mostov, K. (2007). PTEN-mediated apical segregation of phosphoinositides controls epithelial morphogenesis through Cdc42. Cell **128:** 383–397.

Nelson, B.K., Cai, X., and Nebenfuhr, A. (2007). A multicolored set of in vivo organelle markers for co-localization studies in Arabidopsis and other plants. Plant J. **51:** 1126–1136.

Nemoto, Y., Kearns, B.G., Wenk, M.R., Chen, H., Mori, K., Alb, J.G., Jr., De Camilli, P., and Bankaitis, V.A. (2000). Functional characterization of a mammalian Sac1 and mutants exhibiting substrate-specific defects in phosphoinositide phosphatase activity. J. Biol. Chem. **275:** 34293–34305.

Nishio, M., et al. (2007). Control of cell polarity and motility by the PtdIns(3,4,5)P3 phosphatase SHIP1. Nat. Cell Biol. **9:** 36–44.

Novick, P., Osmond, B.C., and Botstein, D. (1989). Suppressors of yeast actin mutations. Genetics **121:** 659–674.

Pendaries, C., Tronchere, H., Racaud-Sultan, C., Gaits-Iacovoni, F., Coronas, S., Manenti, S., Gratacap, M.P., Plantavid, M., and Payrastre, B. (2005). Emerging roles of phosphatidylinositol monophosphates in cellular signaling and trafficking. Adv. Enzyme Regul. **45:** 201–214.

Pinal, N., Goberdhan, D.C., Collinson, L., Fujita, Y., Cox, I.M., Wilson, C., and Pichaud, F. (2006). Regulated and polarized

PtdIns(3,4,5)P3 accumulation is essential for apical membrane morphogenesis in photoreceptor epithelial cells. Curr. Biol. **16:** 140–149.

Preuss, M.L., Schmitz, A.J., Thole, J.M., Bonner, H.K., Otegui, M.S., and Nielsen, E. (2006). A role for the RabA4b effector protein PI-4Kbeta1 in polarized expansion of root hair cells in *Arabidopsis thaliana.* J. Cell Biol. **172:** 991–998.

Preuss, M.L., Serna, J., Falbel, T.G., Bednarek, S.Y., and Nielsen, E. (2004). The Arabidopsis Rab GTPase RabA4b localizes to the tips of growing root hair cells. Plant Cell **16:** 1589–1603.

Rudge, S.A., Anderson, D.M., and Emr, S.D. (2004). Vacuole size control: Regulation of PtdIns(3,5)P2 levels by the vacuole-associated Vac14-Fig4 complex, a PtdIns(3,5)P2-specific phosphatase. Mol. Biol. Cell **15:** 24–36.

Schiefelbein, J.W., and Somerville, C. (1990). Genetic control of root hair development in *Arabidopsis thaliana.* Plant Cell **2:** 235–243.

Schnepf, E. (1986). Cellular polarity. Annu. Rev. Plant Physiol. **37:** 23–47.

Schorr, M., Then, A., Tahirovic, S., Hug, N., and Mayinger, P. (2001). The phosphoinositide phosphatase Sac1p controls trafficking of the yeast Chs3p chitin synthase. Curr. Biol. **11:** 1421–1426.

Sciorra, V.A., Audhya, A., Parsons, A.B., Segev, N., Boone, C., and Emr, S.D. (2005). Synthetic genetic array analysis of the PtdIns 4-kinase Pik1p identifies components in a Golgi-specific Ypt31/rab-GTPase signaling pathway. Mol. Biol. Cell **16:** 776–793.

Varnai, P., and Balla, T. (2007). Visualization and manipulation of phosphoinositide dynamics in live cells using engineered protein domains. Pflugers Arch. **455:** 69–82.

Vincent, P., Chua, M., Nogue, F., Fairbrother, A., Mekeel, H., Xu, Y., Allen, N., Bibikova, T.N., Gilroy, S., and Bankaitis, V.A. (2005). A Sec14p-nodulin domain phosphatidylinositol transfer protein polarizes membrane growth of *Arabidopsis thaliana* root hairs. J. Cell Biol. **168:** 801–812.

Voigt, B., et al. (2005b). Actin-based motility of endosomes is linked to the polar tip growth of root hairs. Eur. J. Cell Biol. **84:** 609–621.

Voigt, B., Timmers, A.C., Samaj, J., Muller, J., Baluska, F., and Menzel, D. (2005a). GFP-FABD2 fusion construct allows in vivo visualization of the dynamic actin cytoskeleton in all cells of Arabidopsis seedlings. Eur. J. Cell Biol. **84:** 595–608.

Wang, X., Cnops, G., Vanderhaeghen, R., De Block, S., Van Montagu, M., and Van Lijsebettens, M. (2001). AtCSLD3, a cellulose synthase-like gene important for root hair growth in arabidopsis. Plant Physiol. **126:** 575–586.

Wei, H.C., Sanny, J., Shu, H., Baillie, D.L., Brill, J.A., Price, J.V., and Harden, N. (2003). The Sac1 lipid phosphatase regulates cell shape change and the JNK cascade during dorsal closure in Drosophila. Curr. Biol. **13:** 1882–1887.

Williams, M.E., Torabinejad, J., Cohick, E., Parker, K., Drake, E.J., Thompson, J.E., Hortter, M., and Dewald, D.B. (2005). Mutations in the Arabidopsis phosphoinositide phosphatase gene SAC9 lead to overaccumulation of PtdIns(4,5)P2 and constitutive expression of the stress-response pathway. Plant Physiol. **138:** 686–700.

Zerial, M., and McBride, H. (2001). Rab proteins as membrane organizers. Natl. Rev. **2:** 107–117.

Zhong, R., Burk, D.H., Nairn, C.J., Wood-Jones, A., Morrison III, W.H., and Ye, Z.H. (2005). Mutation of SAC1, an Arabidopsis SAC domain phosphoinositide phosphatase, causes alterations in cell morphogenesis, cell wall synthesis, and actin organization. Plant Cell **17:** 1449–1466.

Zhong, R., and Ye, Z.H. (2003). The SAC domain-containing protein gene family in Arabidopsis. Plant Physiol. **132:** 544–555.